ISSN 2411-3336; e-ISSN 2541-9404

JOURNAL OF MINING INSTITUTE
Zapiski Gornogo instituta
Journal homepage: pmi.spmi.ru

Research article

A new diamond find and primary diamond potential of the Chetlas uplift (Middle Timan)

Aleksandr M. PYSTIN[1]✉, **Yurii V. GLUKHOV**[1], **Aleksandr A. BUSHENEV**[2]
[1] *N.P.Yushkin Institute of Geology Komi SC UB RAS, Syktyvkar, Russia*
[2] *Republican Center for the Functioning of Specially Protected Natural Areas and Nature Management, Syktyvkar, Russia*

How to cite this article: Pystin A.M., GlukhovYu.V., Bushenev A.A. A new diamond find and primary diamond potential of the Chetlas uplift (Middle Timan). Journal of Mining Institute. 2023. Vol. 264, p. 842-855. EDN GSTWEZ

Abstract. In the previously poorly studied southeastern part of the Chetlas uplift in the Middle Timan, a new occurrence of diamond satellite minerals and a diamond grain were found in the modern channel sediments of the Uvuy River basin. In order to assess the prospects of the area under consideration for identification of diamondiferous objects of practical interest, a characteristic of chromium-bearing pyropes and chromospinelides as the main kimberlite of diamond satellite minerals are given and the diamond grain itself is described. The material for the research was 16 schlich samples, each with a volume of 8 to 15 l. The minerals were studied using optical and scanning electron microscopy, Raman spectroscopy, laser luminescence and X-ray diffraction (Debye – Sherrer method). It is shown that among the pyropes, most of which correspond in composition to minerals of the lherzolite paragenesis, there are varieties belonging to the dunite-harzburgite paragenesis, including those belonging to diamond phase stability regions. Among the studied chromospinelides, chrompicotites and aluminochromites similar in composition to those found in rocks such as lherzolites and harzburgites, as well as in kimberlites, were identified. A diamond grain found in one of the samples has the form of a flattened intergrowth with distinct octahedron faces, complicated by co-growth surfaces with other mineral grains that have not been preserved to date. The discovery of the diamond and the established signs the formation of aureoles of the diamond satellites minerals in the channel sediments of the studied area open up the prospects for discovering their primary sources here.

Keywords: Middle Timan; Chetlas uplift; Upper Devonian; ring structure; modern channel sediments; pyrope; diamond

Received: 23.09.2022 ***Accepted: 23.03.2023*** ***Online: 23.06.2023*** ***Published: 25.12.2023***

Introduction. The Chetlas uplift in Timan is considered to be one of the most promising for the discovery of diamondiferous primary sources [1-2]. This conclusion is based on the finds of diamond satellite minerals (DSM) and diamonds themselves in the modern alluvium of the Kosyu and Nizhnyaya Puzla Rivers, as well as the establishment of the direct signs of kimberlite-lamproite magmatism in the basin of the river Kosyu, due to the works of the 50-80s of the last century, associated with the names of Yu.P.Ivensen, M.I.Osadchuk, Yu.D.Smirnov, N.A.Rumyantseva, V.G.Cherny, R.S.Kontarovich, and many other geologists [3, 4]. In addition, V.G.Cherny discovered a small diamond fragment in lamprophyre schlich from a borehole drilled in the Kosyu exploration area (the Kosyu River basin) [5], and T.G.Shumilova et al. [6] established graphite pseudomorphosis by diamond in carbonatites of the Kosyu massif. Nevertheless, the problem of primary sources of diamond in this area and in the Timan as a whole remains unresolved.

Material on the geology and mineral resources of the Timan, including the Middle Timan, was summarized over the past decade [7]. New data on the age of intrusive rocks [8-10] and stratified deposits [11-13] were obtained. A large amount of mineralogical research was carried out, especially on the well-known Ichetyu diamond occurrence, located to the east of the Chetlas uplift on the Volsk-Vymskaya ridge [14-16]. In this case, the main attention, along with diamond, is paid to zircon and

Journal of Mining Institute. 2023. Vol. 264. P. 842-855

rutile associated with it [17-19]. New data on the lithological composition and mineralogical features of the diamondiferous deposits of the South Timan were obtained [20]. In predicting the diamond content of both platform [21-23] and folded [24, 25] areas, positive experience was gained in using the typomorphic features of the diamond kimberlite satellites (pyropes, chromospinelides, picroilmenites, etc.), which form schlich flows in the fields of productive magmatism development. Exploration models of primary diamond deposits were developed, including those of the north of the East European Platform [26]. Alternative ideas about the diamond genesis are being developed [20, 27]. All of this creates the prerequisites for continuing work on the diamond theme, including solving the problem of primary sources of Timan diamonds.

In 2017, the ring structures of the central type were established in the south-eastern part of the Chetlas uplift [28]. They were identified based on the study of stock and published geological and geophysical materials and additional work performed on the interpretation of satellite images using the method of tubular bodies diagnosticsdeveloped at VSEGEI [29]. Elements of the ring structure are distinguished by different phototone, coloring, photo drawing, and configuration of the hydronetwork. There is a sharp disappearance of straight lineaments (presumably faults) near the contours of the rings.

Taking into account the different geological position of the ring structures, it can be assumed that they can be formed by different-age tubular bodies. Most of the ring structures are spatially associated with areas of the Upper Devonian volcanogenic-sedimentary strata (Fig.1). This may indicate the possibility of an age correlation with the strata of the supposed tubular bodies that formed the ring structures. Possible explosion pipes are associated with the central parts of the isolated ring structures, which have a figure close to a circle, up to 1000 m in diameter, in their central parts. The marginal parts of the ring structures may be a reflection of the formation of metasomatic aureoles around kimberlite pipes or associated with tectonic faults formed during the intrusion of pipes.

In 2017 and 2018, the authors of the article carried out schlich sampling of modern channel sediments of some watercourses in two sites in the area of development of the most numerous group of ring structures, which is called the Uvyu group (Fig.1). In all but one of the samples, pyrope grains were found, and in one of the samples, when examining the heavy non-magnetic fraction of the concentrate under a microscope binocular stereoscopic (MBS-9) with ultraviolet illumination, a diamond grain was found. In general, among the minerals associated with pyropes, garnets of various compositions, staurolite, amphiboles, kyanite, rhombic and monoclinic pyroxenes (including chromium diopsides), epidote, ilmenite, rutile, zircon dominate in the sample concentrates; chromospinelides, noble spinel, corundum are noted, cordierite, apatite, baddeleyite, loparite, wustite, perovskite, titanite, pyrite, chalcopyrite, native gold is occasionally found.

Brief information on the results of mineralogical studies of schlich samples is given in the article [30]. The results of this work are presented in more detail in this publication, which aims to contribute to giving a new impetus to initiative and prospecting for diamonds in the Middle Timan, including, among other things, new, previously poorly studied areas of this region.

Research methods and material. Schlich samples were taken from modern (Holocene) channel sandy and sandy-gravel sediments of the Uvyu River and its right-bank tributaries, mainly upstream from the mouth of the stream Gnilaya Uvyu (a right-bank tributary of the Uvyu river), as well as an unnamed left-bank tributary of the Mezen River, which flows 8 km above the mouth of the Uvyu River, in the locality Izby Ozerki (Fig.1). A total of 16 samples were taken with a volume of 8 to 15 l each, including 14 samples from the channel sediments of the Uvyu River and its tributaries (site A) and two samples from the channel sediments of a nameless stream in the locality Izby Ozerki (site B). Samples were taken both on the shallows and in the near-stream parts of the mentioned water bodies to a depth of no more than 0.2-0.3 m from the sediment surface.

Journal of Mining Institute. 2023. Vol. 264. P. 842-855 EDN GSTWEZ

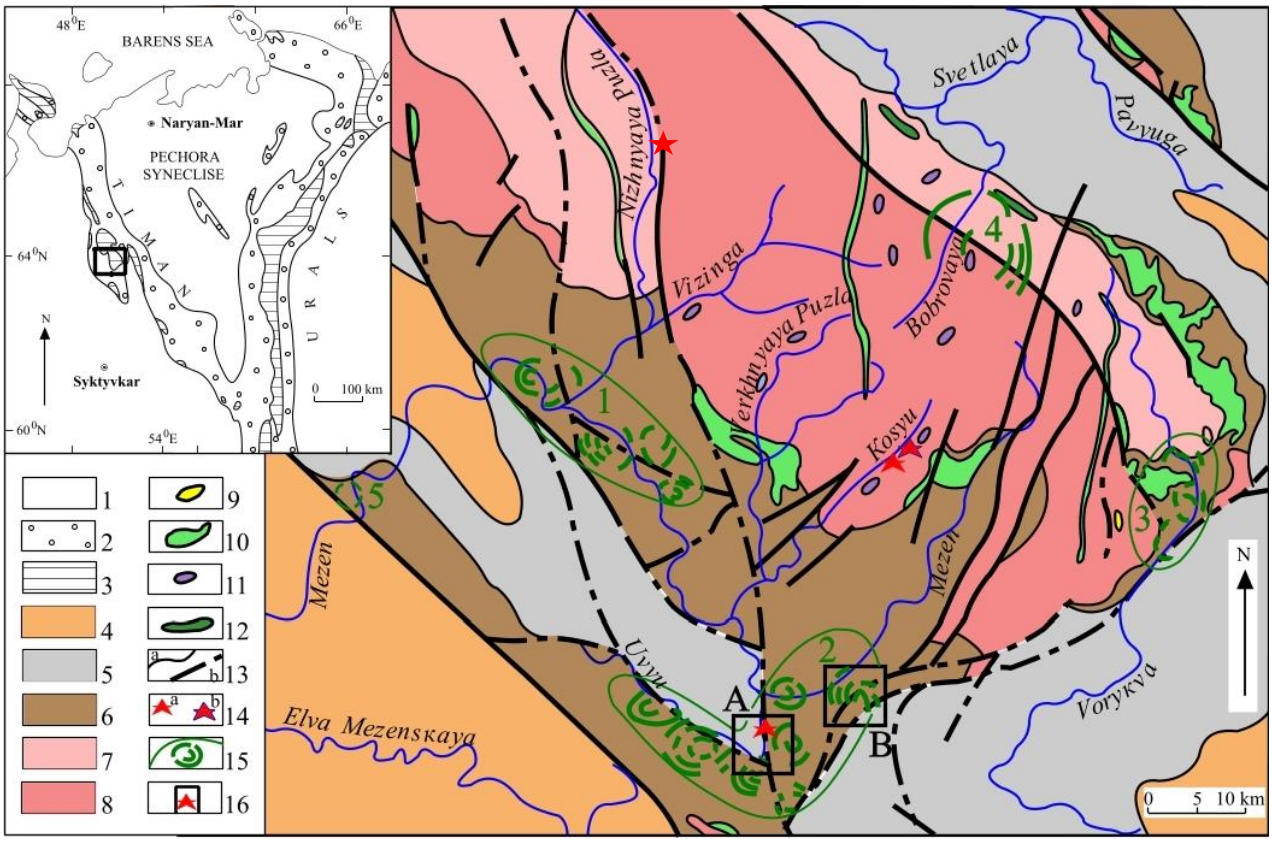

Fig.1. Scheme of arrangement of ring structures in the southeastern part of the Chetlas uplift (Middle Timan). Compiled based on the materials of geological surveys, taking into account the data from the interpretation of satellite images

Inset 1-3: 1 – Meso-Cenozoic platform cover; 2 – Paleozoic complexes; 3 – Precambrian complexes; the square marks the south-eastern part of the Chetlas uplift; on the scheme 4-16: 4 – Permian deposits, undivided (limestones, dolomitic limestones and dolomites); 5 – Carboniferous deposits, undivided (limestones, dolomitic limestones and dolomites); 6 – Upper Devonian deposits, undivided (sandstones, silt-clay shales, tuffs); 7, 8 – deposits of the Upper Riphean: 7 – Bysrinskaya series (dolomites, dolomitic limestones, sandstones and siltstones with members of clayey shales and interlayers of gravelstones and conglomerates; in the lower part of the section – thin (up to 3 m) conformable bodies of metatuffs and metatuffites of the basic composition), 8 – Chetlas series (chlorite-sericite-quartz shales, silt schists, siltstones, quartzite sandstones and quartzites); 9-12 – igneous complexes: 9 – Early Permian high-potassium trachytes, 10 – Late Devonian dolerite-basalt, 11 – Late Riphean-Vendian alkaline picrites, lamprophyres (biotite-phlogopite rocks), 12 – Late Riphean metadolerite; 13 – geological boundaries: a – boundaries of stratigraphic units and intrusive bodies; b – faults; 14 – known finds of diamonds: a – in modern alluvial deposits, b – in alkaline ultrabasic rocks; 15 – ring structures; 16 – areas of sampling works (asterisk shows the location of the sample with a diamond grain); green numbers indicate groups of ring structures (1 – Mezenskaya, 2 –Uvyu, 3 – Vorykvinskaya) and single ring structures (4 – Bobrovskaya, 5 – Kipreyskaya)

When studying samples, the main attention was focused on the presence and quantitative content of pyrope as the main (DSM), as well as to the search for diamond itself (Table 1). Elevated (8 or more grains per 10 l of sample) contents of pyrope grains were established in three samples taken in the near-stream part of the Uvyu River. In one of them, the richest in pyropes (sample 36), a diamond grain was found. Chromospinelides were isolated and studied in this sample. In the rest of the samples taken from the channel sediments of the Uvyu River and its tributaries, the content of pyrope grains varies from 1 to 6 grains per 10 l of sample. In the samples taken from the channel sediments of a nameless stream in the locality Izby Ozerki, sources of which go around the central contour of one of the ring structures of the Uvyu group, the maximum content of pyrope is 6 grains per 10 l of the sample.

Laboratory studies of minerals were carried out on the base of the Collective Use Center "Geo-science" of the Institute of Geology FRC Komi Scientific Center of the Ural Branch of the Russian Academy of Sciences. The results of the study of pyrope as the main (DSM), chromospinelides and

Journal of Mining Institute. 2023. Vol. 264. P. 842-855

the first diamond found in the alluvium of the river Uvyu were presented. The photographic images of mineral grains were obtained using optical microscopes MBS-9 (digital camera Sony Cyber-shot DSC-W830), NikonEclipse LV100ND (digital camera DS-L3). Ultraviolet illumination was provided by a DRK-120 lamp. The surface details and elemental composition were studied using a Tescan VEGA 3 LMN scanning electron microscope with an INCA Energy 450 energy dispersive spectrometer and an EBSD attachment (operating voltage 20 kV, sputtering with carbon).

The most typical chemical compositions of minerals are given. Raman scattering (RS) and laser luminescence (LL) spectra of diamond were recorded on a LabRam HR800 spectrometer (HoribaJobinIvon), excitation by red (λ_{ex} = 633 nm) and green (λ_{ex} = 488 nm) lasers, the sample temperature was 300 K. The structural characteristics of the diamond were obtained using equipment for X-ray diffraction analysis on an ARSF device (X-ray sharp-focus apparatus), Cu-anode, current 10 mA, voltage 30 kV, no filtering was carried out, Debye – Sherrer chamber (radius 28.65 mm) was also used. The unit cell parameters were calculated by the least squares method.

Results and discussion. *Pyropes.* Pyrope has been identified and isolated in concentrates of all schlich samples except for sample 31. The mineral is characterized mainly by purple color and has various color shades (including reddish, pinkish, violet) and color saturation (Fig.2). The maximum size of pyropes ranges from 0.24 to 0.61 mm. Their average geometricsizes vary from 0.13 to 0.33 mm, the corresponding size classes are from +0.1 to +0.25 and from +0.25 to +0.5 mm.

Pyrope individuals are characterized by an elongated flattened grain shape, a rounded-angular or angular-rounded appearance (Fig.2) and do not possess, as a rule, the crystallographic shapes of the garnet group minerals.

In a sample of pyrope garnets there are quite a lot of rounded grains. It is supposed that formation of different in shape garnet grains (from spherical to flattened oval) can occur in endogenous settings during melting as a result of the interaction of minerals with kimberlite melt [31]. Among pyrope garnets, there are also specimens with specific sharp-edged morphology and curvilinear surfaces (Fig.2, *e*, *s*, *v*), which are described as cuboids in the literature devoted to the mineral companions of diamond [22, 31].

Table 1

The content of pyrope and diamond in schlich samples

Sample number	Sample volume, l	View results	
		Pyrope, pcs.	Diamond, pcs.
Site A			
12	10	3	0
13	10	1	0
27	7	2	0
28	8	1	0
31	10	0	0
32	10	2	0
33	7	8	0
36	15	22	1
37	15	6	0
38	10	4	0
41	10	15	0
42	10	3	0
43	10	4	0
44	10	1	0
Site B			
39	10	2	0
40	10	6	0

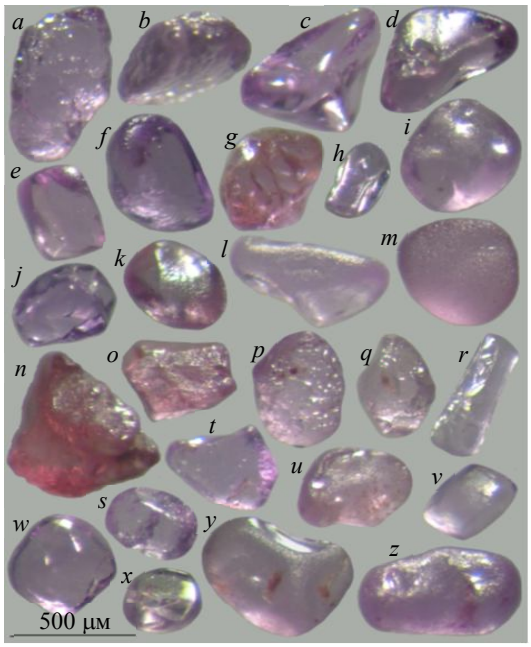

Fig.2. Morphology and surface of pyropes (optical microscope MBS-9): *a-m* – pyrope grains from sample 36, in which diamond was found. Typomorphic elements of morphology and surface of pyropes: *e*, *s*, *v* – cuboids; *c*, *d*, *f-i*, *k*, *m*, *w*, *x* – ovalization; *c*, *d*, *g-i*, *k*, *s*, *w*, *x* – mirror shine; *a*, *b*, *f*, *o*, *q*, *s* – tuberosity (bubbly); *p* – shingles; *h*, *j*, *n*, *o*, *r*, *t*, *w*, *y* – chipped grains; *d*, *i*, *r*, *u*, *z* – pothole; *e*, *o* – unworn rib; *d*, *g*, *i-m*, *s-w*, *y*, *z* – matting of the worn edge and sides of the grain; *p*, *q*, *t*, *u*, *y*, *z* – brown pigment spots

As was established earlier [31], pyrope cuboids are the limiting forms of hypergene dissolution. However, it can be assumed that cuboids can occur not only in intermediate reservoirs, but also in eroded and eluted upper parts of kimberlite bodies. The surface of pyrope grains that were not subjected to intense exogenous mechanical wear that occurs during transportation retained a diverse specific microrelief – shingles (Fig.2, *p*), tuberculate-bubbly (Fig.2, *a*, *b*, *f*, *o*, *q*, *s*), etc. Examination of pyrope grains under an optical microscope often reveals a characteristic high specular luster (Fig.2, *c*, *d*, *g-i*, *k*, *s*, *w*, *x*). The comparison of morphology and surface of pyropes that were not subjected to intense exogenous mechanical wear from the schlich samples at our disposal with pyropes from the upper eluted part of the Vodorazdelnaya pipe (Middle Timan, Volsk-Vymskaya ridge, Umba kimberlite field) indicates their similarity. On the surface of some grains there are pigmented brown spots (Fig.2, *p*, *q*, *t*, *u*, *y*, *z*). Possibly it is "shine through" undiscovered mineral inclusions. Mineral inclusions of chromospinelides, orthopyroxene (enstatite), and iron-magnesian micas were found in pyropes similar in appearance (Table 2). In one case, the pyrope surface shows kelyphitic-like fragmentary outgrowths with unclear mineral content of the carbon-bearing phase and chalcopyrite microexcretions.

Table 2

Composition of microinclusions in pyrope garnets and chromespinels, wt.%

Number in order	Component									Sum	Mineral
	SiO_2	TiO_2	Al_2O_3	Cr_2O_3	FeO	MgO	CaO	K_2O	Na_2O		
1	58.30	–	1.26	0.36	4.06	37.08	0.20	–	–	101.26	Orthopyroxene (enstatite) $(Mg_{1.88}Fe_{0.11}Ca_{0.01})_2(Si_{1.94}Al_{0.05}Cr_{0.01})_2O_6$
2	57.82	–	1.14	0.42	3.85	36.66	0.16	–	–	100.05	Orthopyroxene (enstatite) $(Mg_{1.88}Fe_{0.11}Ca_{0.01})_2(Si_{1.94}Al_{0.05}Cr_{0.01})_2O_6$
3	56.78	–	1.28	0.43	4.95	35.72	0.30	–	–	99.46	Orthopyroxene (enstatite) $(Mg_{1.85}Fe_{0.14}Ca_{0.01})_2(Si_{1.94}Al_{0.05}Cr_{0.01})_2O_6$
4	39.71	0.52	16.36	0.34	16.20	4.41	0.87	3.20	0.44	82.05	Iron-magnesian mica $(K_{0.31}Na_{0.06})_{0.37}(Fe_{1.02}Mg_{0.49}Al_{0.45}Ca_{0.07}Ti_{0.03}Cr_{0.02})_{2.08}AlSi_3O_{10}(OH, F)_2$
5	47.89	4.43	3.95	1.28	7.24	17.79	18.95	0.13	0.56	102.22	Clinopyroxene (diopside) $(Mg_{0.98}Ca_{0.75}Fe_{0.22}Na_{0.04}K_{0.01})_2(Si_{1.68}Al_{0.16}Ti_{0.12}Cr_{0.04})_2O_6$
6	36.87	6.73	3.96	8.57	10.75	14.83	16.65	0.24	0.45	99.05	Clinopyroxene (diopside) $(Mg_{0.88}Ca_{0.71}Fe_{0.36}Na_{0.04}K_{0.01})_2(Si_{1.38}Cr_{0.25}Ti_{0.19}Al_{0.18})_2O_6$
7	38.57	0.75	19.12	0.88	14.75	15.58	–	7.53	–	97.18	Iron-magnesian mica $K_{0.75}(Fe_{0.96}Mg_{1.81}Al_{0.75}Ti_{0.04}Cr_{0.05})_{3.61}AlSi_3O_{10}(OH, F)_2$
8	51.16	0.78	4.95	0.92	3.79	16.99	21.72	–	0.42	100.73	Clinopyroxene (diopside) $(Mg_{0.96}Ca_{0.89}Fe_{0.12}Na_{0.03})_2(Si_{1.76}Al_{0.20}Ti_{0.02}Cr_{0.02})_2O_6$
9	–	–	–	0.68	5.53	17.33	28.47	–	–	52.01	Dolomite Ca $(Mg_{0.85}Fe_{0.15})(CO_3)_2$

Notes. All analyzes refer to sample 36; numbers 1-4 – inclusions in pyrope garnets, 5-9 – inclusions in chromespinels.

Pyropes subjected to exogenous mechanical wear shows specific matting of edges or sides of grains (Fig.2, *d*, *g*, *i-m*, *s-w*, *y*, *z*). Examination of the surface under an electron microscope shows that it is replete with chaotically arranged heterogeneous pits of mechanical damages. Mechanical wear of pyrope grains could occur during transportation, both in modern watercourses and at the stage of possible formation of intermediate reservoirs. Note, that at the end of the 1980s in the southern part of the Obdyr uplift, located several tens of kilometers to the southeast of the studied area, in the basal terrigenous sequence of the Visean-Serpukhovian section, during specialized works in search of primary diamond sources conducted under the direction of L.P.Bakulina, DSM – pyropes, picroilmenites and chromospinelides were found. In the Chetlas uplift, basal terrigenous deposits of this age level belong to the Timsher suite, which occurs with a stratigraphic break on various Upper Devonian horizons, and in fragments with erosion on metamorphic formations of the Upper Proterozoic.

Journal of Mining Institute. 2023. Vol. 264. P. 842-855

The study of the chemical composition features of 80 pyrope grains isolated by us (according to 97 local analyzes) shows that the general range of MgO concentrations in the mineral varies from 17 to 24 wt.%. The corresponding range of the calculated pyrope component contents is 48.7-77.9 %. There is no zoning in the distribution of magnesium in garnet grains. The Cr_2O_3 content in them varies from 0.9 to 8.7 wt.%. Approximately 20 % of the analyzed pyrope grains show zonality in distribution of chromium – the concentration of this element decreases from the center to the edge. The amount of the knorringite minal is 2.9-24.9 %. The FeO content in pyropes – 6.4-10.8 wt.%, which corresponds to 12.7-21.4 % of the almandine minal, and the amount of CaO – 1.23-7.12 wt.% (3.1-18.2 % of the grossular minal).

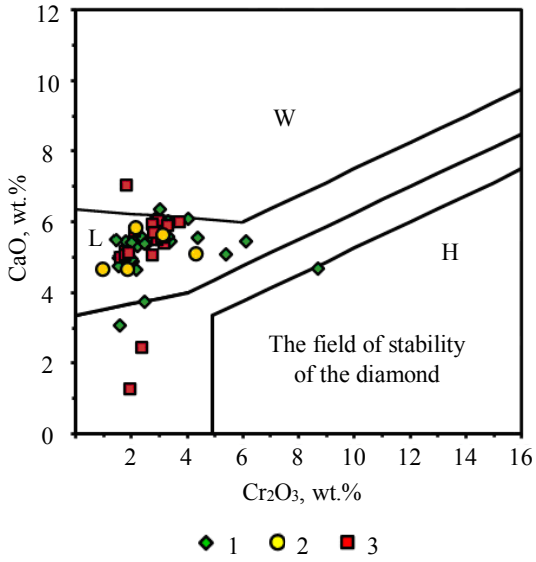

Fig.3. Compositions of purple chromium-containing pyropes of the Uvyu River and its tributaries (1), an unnamed stream in the locality Izby Ozerki (2) and diamond-bearing sample 36 from the mouth of the Uvyu River (3) in the fields of pyrope garnets of various parageneses on the diagram by N.V.Sobolev [35]

W – wehrlites; L – lherzolites; H – dunites and harzburgites

Differences in pyrope magnesium content are probably associated with their original belonging to different parental rocks, and in concentration of chromium and calcium, moreover, with the possible manifestation of metasomatism [32-34]. A small amount of manganese (0.2 to 0.8 wt.% MnO) is constantly registered among minor impurities in pyrope. The corresponding calculated contribution of the spessartine component does not exceed 1.5 %. The presence of titanium (up to 0.86 wt.% TiO_2) is sporadically detected in pyropes; in one case traces of scandium (0.15 wt.% Sc_2O_3) are recorded.

The figurative points of pyrope compositions are shown in N.V.Sobolev's discriminant diagram (Fig.3). The diagram was constructed using local analyzes of all isolated pyrope grains. Typical compositions of pyropes that can be attributed to various rock parageneses are given in Table 3.

In the discriminant diagram the figurative points of the compositions of the most pyrope analyses form a compact “swarm” of points for chromium and calcium, which is in a narrow range of values – 1.2-4.0 wt.% Cr_2O_3 and 4.3-6.1 wt.% CaO in the lherzolite field and partially crosses the upper boundary of this field. The main group is joined by two small groups of pyropes creating two compositional trends. One such group shows a significant variation in calcium, with relatively constant chromium concentrations. This and the main group include all pyropes from sample 36 in which the largest amount of this mineral was found and a diamond was detected. In the second group, on the contrary, there is a noticeable variation in chromium with a certain constancy of calcium content. The vast majority of the studied pyropes belong to the lherzolite paragenesis. The compositional points of two pyropes with a high calcium content are in the field of wehrlite paragenesis. Several pyrope points with low calcium concentrations were localized in the dunite-harzburgite field. One point of this mineral composition was in the diamond stability field. This distribution of pyrope compositions may be associated with their entry into channel sediments from different sources.

According to the chemical-genetic classification of garnets of the ultramafic and eclogitic parageneses of the Arkhangelsk diamond province [21], most of the available pyropes correspond in composition to garnets from diamond-bearing uniform-grained lherzolites, a smaller part (about 8 %) corresponds to diamond-bearing peridotites with high- and medium-chromium garnet. Moreover, although lherzolite pyropes in the Arkhangelsk diamondiferous province actually are not a sign of diamond-rich pipes, this group of garnets is found in them quite often [23].

Table 3

Chemical composition of garnets, wt.%

Component	Grain number						
	36/1		36/12		36/18		41/1
	c	*r*	*c*	*r*	*c*	*r*	–
SiO_2	41.54	41.55	41.72	41.81	42.69	42.52	41.09
Al_2O_3	22.42	22.78	22.44	22.80	23.07	23.16	17.61
Cr_2O_3	1.94	1.73	1.92	1.88	2.05	1.89	8.69
FeO	8.12	7.84	7.71	7.86	7.11	6.98	7.00
MnO	0.40	0.47	0.32	0.37	0.39	0.26	0.29
MgO	18.70	18.78	20.34	20.41	23.95	23.89	20.74
CaO	7.12	6.97	5.12	5.10	1.29	1.23	4.69
Sum	100.26	100.12	99.57	100.23	100.55	99.93	100.11
Si^{4+}	2.975	2.973	2.983	2.972	2.981	2.982	2.978
Ti^{4+}	0.000	0.000	0.000	0.000	0.000	0.000	0.000
Al^{3+}	1.890	1.918	1.889	1.907	1.896	1.912	1.502
Fe^{3+}	0.000	0.000	0.000	0.000	0.000	0.000	0.000
Cr^{3+}	0.110	0.098	0.108	0.105	0.113	0.105	0.497
Fe^{2+}	0.486	0.468	0.460	0.467	0.415	0.409	0.424
Mn^{2+}	0.024	0.028	0.019	0.022	0.023	0.015	0.018
Mg^{2+}	1.994	2.000	2.166	2.160	2.490	2.495	2.238
Ca^{2+}	0.546	0.534	0.392	0.388	0.097	0.092	0.364
Alm	16.2	15.6	15.3	15.6	13.8	13.6	14.1
Sps	0.8	0.9	0.6	0.7	0.8	0.5	0.6
Grs	18.2	17.8	13.1	12.9	3.2	3.1	12.1
Py	60.0	60.8	65.8	65.7	76.3	77.9	48.7
Knor	5.5	4.9	5.4	5.3	5.7	5.2	24.9
Sum	100.7	100.0	100.3	100.2	99.8	100.4	100.5

Notes. Analyzes 36/1 refer to the wehrlite, 36/12 – to the lherzolite, 36/18, 41/1 – to the dunite-harzburgite paragenesis; *c* – center and *r* – grain rim.

Chromospinelides. In schlich samples the spinel group minerals grains, represented mainly by chromospinelides, are easily recognizable by their characteristic octahedral habitus, resinous black color (sometimes with a brownish tinge), and conchoidal fracture with a vitreous luster. The grain size varies from 0.15 to 0.6 mm and is usually set in particle size classes from +0.1 to +0.25 and from +0.25 to +0.5 mm.

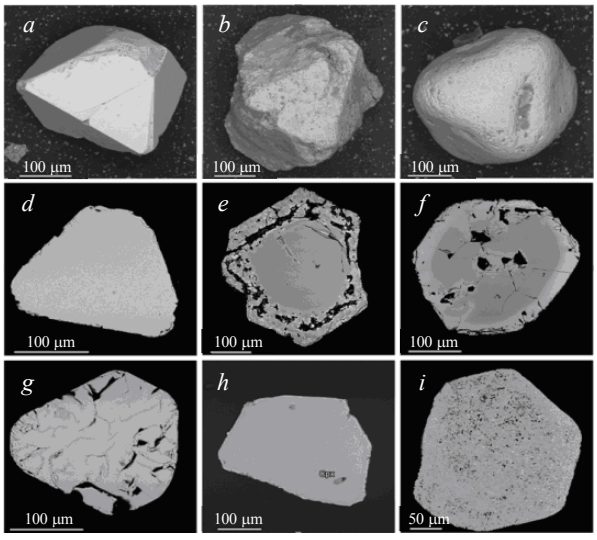

Fig.4. Morphology, internal structure and microinclusions of chromospinelides (scanning electron microscope Tescan VEGA 3LMN: back-scattered electrons)

Morphologically chromospinelides are represented by rounded-angular, angular, and angular-comminuted grains (Fig.4). The octahedral habitus is clearly distinguishable only in half of the specimens. In addition to the octahedron faces, there are faces of the rhombic-dodecahedron, less often faces of other simple shapes. Rare twin aggregates are present. Some chromospinelide grains clearly show a corrosion microrelief (Fig.4, *b*).

The grains of the spinel group are clearly distinguished from one another by their internal structure, which correlates with the features of their composition and partly with their morphology. There are two main groups of grains.

Journal of Mining Institute. 2023. Vol. 264. P. 842-855

The first most numerous group (up to two thirds of the entire sample, comprising 34 grains) is represented by euhedral octahedral crystals of chromospinelides (Fig.4, *a-c*), which stand out from the total mass with a characteristic blue-black color. They are relatively large in size, and weakly rounded in terms of roundness. The morphological specificity of this group is the increased occurrence of anhedral comminuted individuals (up to half of the specimens), and the presence of single well-rounded grains (Fig.4, *c*). The vast majority of chromospinelides of this group have a homogeneous internal structure (Fig.4, *d*). In single examples a thin epigenetic rim is visible on grain sections (Fig.4, *e*, *f*), which sharply borders on the inner region of the grain. In the rim, as a rule, the content of iron is higher (contribution of magnetite minal) and the content of magnesium and aluminum is lower (contribution of spinel minal). In some cases, the characteristic pitting of dissected sections reveals individuals with a specific crack-block structure (Fig.4, *g*), the cause of which, obviously, is in the stressed state of the crystalline grain, which causes its fragility. Quite often mineral inclusions occur in chromospinelides (Fig.4, *h*).

Table 4 shows only the most typical compositions of the analyzed chromospinelides. The compositions of the entire sample of chromospinelides (excluding specimens significantly enriched in titanium) are placed on the combined Al^{3+}-Cr^{3+}-Fe^{3+}-Mg^{2+}-Fe^{2+}trigonogram (Fig.5). Taking into account 50 analyzes of this mineral that we have obtained, it has been established that the main part of chromospinelide grains varies from the varieties enriched with spinel component (chrompicotite, including more ferruginous subferrichrompicotite) to those that are significantly enriched in chromite minal (alumochromite, including more ferruginous subferrialumochromite). These varieties of chromospinelides are characterized by the periodic presence of a small admixture of titanium, (0.2-0.8 wt.% TiO_2), vanadium (0.2-0.5 wt.% V_2O_3) and zinc (0.3-6.9 wt.% ZnO). Traces of nickel (0.3 wt.% NiO) and manganese (0.6 wt.% MnO) were found in the mineral composition in isolated cases. In this group there are also specimens with a high proportion of chromite and magnetite end-members – chromites and chromomagnetites (including ferrichromite, subaluminoferrichromite, subaluminochromitemagnetite, ferrialuminochromite). Like other chromospinelides they have a characteristic black color and a greasy sheen. Morphologically and anatomically, they are similar to the described chrompicotites and alumochromites; however, the chromites and chromium magnetites are clearly more rounded (Fig.4, *c*). Another distinguishing feature of chromites and chromium magnetites is expressed in their smaller size. They were found only in the class from +0.1 to +0.25 mm. The ribs and tops of the crystals are significantly worn. They contain titanium (0.3-6.6 wt.% TiO_2), sometimes zinc (0.5-0.9 wt.% ZnO), and sporadically, traces of nickel (0.2-0.4 wt.% NiO), vanadium (0.2-0.3 wt.% V_2O_3), and manganese (0.4-0.9 wt.% MnO).

A specific feature of chrompicotite and alumino-chromite chromospinelides is the relatively frequent occurrence (approximately in every third grain) of silicate microinclusions. One case of dolomite inclusion was also recorded. Silicate inclusions are mainly represented by pyroxenes microphases (clinopyroxenes) as well as silicates similar in composition to micas or amphiboles (specific studies should be carried out to determine mineral identity of their species).

Clinopyroxenes vary in size from 2-3 to 20 μm. In composition they are magnesium-calcium pyroxenes,data on which are satisfactorily calculated for the diopside formula (chromium diopside). They also contain iron (from 3.8 to 10.8 % FeO). Chromium varies from 0.9 to 8.6 wt.% Cr_2O_3. There is also an admixture of titanium from 0.8 to 6.7 wt.% TiO_2. Potassium (0.1-0.2 wt.% K_2O) and sodium (0.4-0.6 wt.% Na_2O) occur as trace impurities in the mineral. Ribbon or layered silicates (mica-like) differ in composition – magnesium-ferrous and iron-magnesium are found. Their characteristic feature is an increased potassium content (3.2-7.5 wt.% K_2O). They contain an admixture of titanium (0.52-0.75 wt.% TiO_2) and chromium (0.34-0.88 wt.% Cr_2O_3). The magnesium-iron silicate inclusion contains an admixture of sodium (0.4 wt.% Na_2O).

Table 4

Chemical composition of chromespinels, wt.%

Component	Grain number							
	1	2	3		4		5	
	–	–	*c*	*r*	*c*	*r*	*c*	*r*
TiO_2	–	0.29	0.38	0.60	0.22	–	–	–
Al_2O_3	28.54	24.20	26.95	28.80	14.95	14.68	9.41	9.46
Cr_2O_3	42.69	43.35	41.19	37.51	47.76	48.05	61.55	60.26
FeO	12.79	18.00	13.25	15.33	33.07	32.11	21.60	22.96
MgO	15.48	13.26	17.43	16.77	3.89	3.72	7.88	6.01
Sum	99.50	99.94*	99.20	99.01	100.40*	99.04*	100.44	99.55*
Type Chsp	AXp	AXp	AXp	СФХП	СФАХ	AXp	Xp	Xp
Component	6		7		8		9	
	c	*r*	*c*	*r*	*c*	*r*	*c*	*r*
TiO_2	0.67	0.65	0.48	0.48	6.56	3.28	0.57	0.53
Al_2O_3	5.29	4.67	37.03	36.76	5.03	5.13	28.93	33.42
Cr_2O_3	56.58	57.07	30.42	29.60	35.47	40.84	38.93	26.78
FeO	26.50	26.38	14.38	15.32	35.39	33.08	16.28	28.90
MgO	10.80	10.32	18.38	18.03	15.61	16.96	16.88	2.67
Sum	100.28*	99.09	101.27*	100.58*	98.58*	99.51*	101.59	99.13*
Type Chsp	СФXp	СФXp	ХПт	СФХП	САХМ	САФХ	СФХП	ХПт
Component	10		11		12		13	
	c	*r*	*c*	*r*	*c*	*r*	*c*	*r*
TiO_2	11.27	6.10	–	–	1.39	3.33	0.18	0.41
Al_2O_3	0.87	0.45	31.06	1.05	14.38	5.03	12.25	0.27
Cr_2O_3	2.15	2.12	37.17	31.18	38.20	34.78	52.79	42.55
FeO	78.41	82.79	18.79	58.02	38.22	50.13	26.09	47.55
MgO	2.42	1.74	13.45	2.16	4.63	2.58	7.96	2.73
Sum	95.54*	93.54*	100.47	93.71	97.50*	96.11*	100.19*	93.97*
Type Chsp	Мгт	Мгт	ХПт	ХМт	ФАХ	САФХ	СФАХ	ФXp

Notes. All analyzes refer to sample 36. Numberes 1, 2 – microinclusions of chromespinels in pyrope garnets. Trace contents of chromospinels were found in grains, wt.%: SiO_2 – 0.25 (6*c*), 0.27 (7*c*), 0.71 (9*r*), 1.30 (11*r*); V_2O_3 – 0.43 (2), 0.51 (4*c*), 0.48 (4*r*), 0.19 (6*c*), 0.42 (10*c*), 0.34 (10*r*), 0.21 (12*c*), 0.26 (12*r*), 0.33 (13*c*), 0.23 (13*r*); MnO – 0.26 (8*c*), 0.59 (13*c*), 0.38 (13*r*); NiO – 0.31 (7*c*), 0.39 (7*r*), 0.26 (8*c*), 0.22 (8*r*); ZnO – 0.41 (2), 0.86 (5*r*), 6.92 (9*r*), 0.47 (12*c*). CP – chromepicotite, AC – aluminochromite, SFAC – subferrialuminochromite, SFCP – subferrichromepicotite, Chr – chromite, FC – ferrichromite, SFC – subferrichromite, SAFC – subaluminoferrichromite, FAC – ferrialuminochromite, SACM – subaluminochromemagnetite, CM – chromemagnetite, Mgt – magnetite [36]. An asterisk marks the amounts taking into account the contents of the above elements. See the rest of the designations in the notes to Table 3.

Microinclusions of chromospinelides in pyropes are represented by chromospineles, which are characteristic of the described group. Their composition is characterized by a relatively high aluminum content (from subferrichrompicotite to aluminochromite). The figurative points of the compositions fall on the trends of chromospineles from ultramafic rocks [37, 38].

The second small population of mineral grains (about a quarter to a third of specimens) from the spinel group are titanomagnetites and magnetites. Titanomagnetites have a characteristic dark gray to black color, often with an iridescent sheen and a slight brownish tint. They are represented by angular, as a rule, euhedral octahedral and rhombicdodecahedral-octahedral individuals with a specific lattice internal structure (Fig.4, *i*). The ribs of such individuals are usually slightly worn. The magnetite component dominates in structure of such spinels. The typical internal structure of titanomagnetites is reticulate, caused by the decomposition of a solid spinel solution into magnetite and ilmenite. Inclusions of albite, quartz and other rock-forming minerals are noted inside the grains. Magnetites of

Journal of Mining Institute. 2023. Vol. 264. P. 842-855

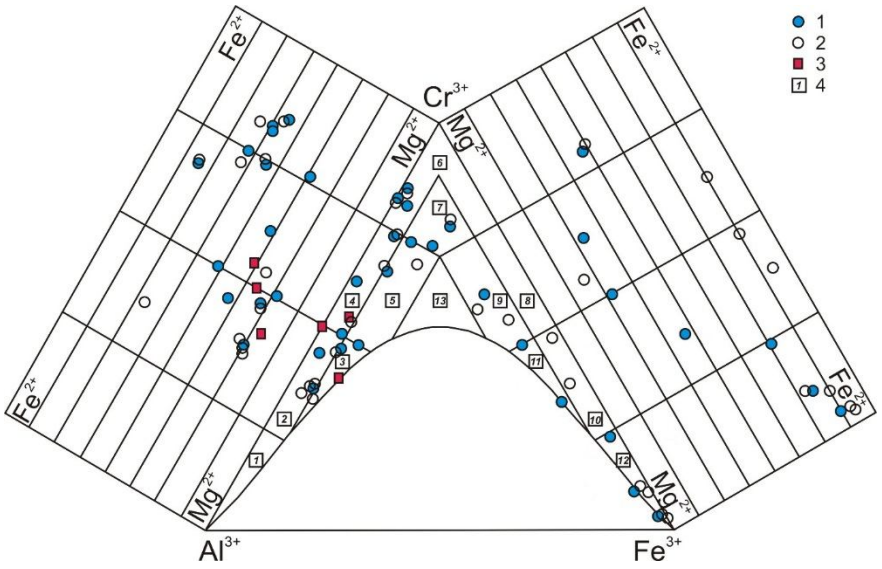

Fig.5. Combined triangular diagram (Al^{3+}-Cr^{3+}-Fe^{3+}-Mg^{2+}-Fe^{2+}) of the Uvyu River chrome spinel compositions

Points and fields of compositions: 1 – unchanged central region of the grain; 2 – grain periphery or areas of epigenetic transformations (border); 3 – inclusions of chrome spinels in parasteresis pyropes; 4 – classification fields of compositions of spinel varieties [36]

1 – picotite; 2 – chrompicotite; 3 – subferrichrompicotite; 4 – aluminochromite; 5 – subferrialumochromite; 6 – chromite; 7 – subferrichromite; 8 – ferrichromite; 9 – subaluminoferrichromite; 10 – chrommagnetite; 11 – subaluminochrommagnetite; 12 – magnetite; 13 – ferrialuminochromite

an octahedral or rhombododecahedral habitus are well identified by their characteristic red-brown tint and porous corroded surface. They vary widely in size, often appearing in several granulometric size classes at once.

Magnetites (including mineral grains similar in composition, formally not included in the boundaries of N.V.Pavlov's diagram [36]) are clearly distinguished in composition by high titanium contents (2.2-11.3 wt.% TiO_2). As in chromospinelides, they contain low contents of nickel (0.4-0.8 wt.% NiO) and vanadium (0.3-0.4 wt.% V_2O_3) and sometimes manganese (1.3-1.9 wt.% MnO).

Petrogenetically chrompicotites, aluminochromites, and similar varieties with a somewhat larger contribution of the magnetite minal are close to rocks lherzolites and harzburgites types [36-38]. Alumochromites together with suferrialumochromites are similar in composition to chromospinelides from kimberlites of the Umba kimberlite field of the Volsk-Vym ridge [5]. The hromites found in the Holocene psephytes of the Uvyu River are typical for dunites [36-38]. Their rare specimens were found in the conglobreccia horizons of the Ichetyu gold-diamond-rare-metal placer and also in the kimberlites of the Umba field [5]. Chrompicotites and alumochromites from psephytes of the river Uvyu have a "fresh" appearance and may have a nearby source. Chromites, on the contrary, are significantly rounded, although perhaps, as in the case of pyropes, their rounding is caused not by-mechanical transportation, but by magmatic processes.

Diamond. It was identified during examining the heavy non-magnetic fractionof concentrates of schlich samples under an MBS-9 binocular microscope with ultraviolet illumination. The diamond grain size is 0.4×0.3×0.1 mm (Fig.6). Under the filtered light of an ultraviolet lamp (DRK-120), diamond stands out against the background of non-luminescent schlich minerals with its pale greenish luminescence (Fig.6, *a*), transparency, diamond luster, and the absence of surface abrasion traces (Fig.6, *b-c*). Under optical and electron microscopes it can be seen that a diamond grain has the form of a flattened crystal with distinguishable octahedral faces, complicated by surfaces of joint growth with other mineral grains that have not been preserved to date.

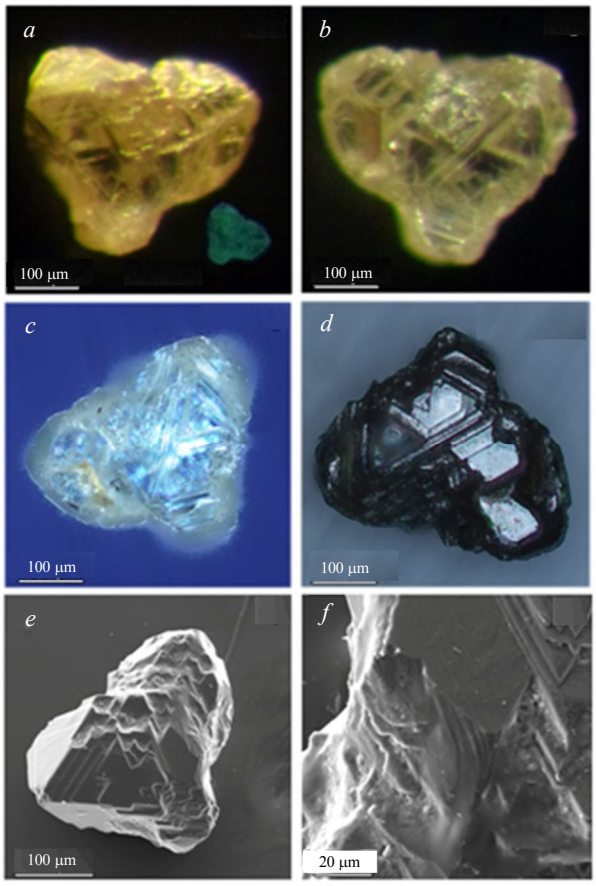

Fig.6. Images of diamond morphology in the MBS-9 optical microscope: *a* – photostimulated luminescence (bottom right), *b* – standard mode; in the optical microscope NikonEclipse LV100ND: *c* – transmission mode, *d* – reflection mode; in the electron microscope TescanVEGA 3 LMN (secondary electrons): *e* – general view, *f* – detail

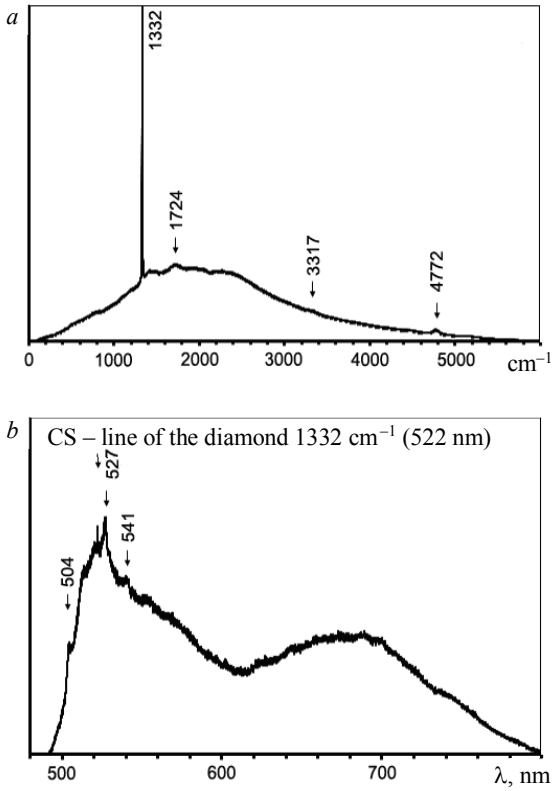

Fig.7. Spectra of diamond (300 K): *a* – Raman spectrum (λ_{ex} = 633 nm); *b* – superposition of the Raman and laser luminescence spectra (λ_{ex} = 488 nm)

On the sides of the diamond, triangular octahedral faces framed by growth steps are clearly distinguishable and combine with faces of other simple shapes (Fig.6, *b-e*). The blocky nature of the diamond is clearly visible on one of the sides (Fig.6, *d*). The layers of the octahedral face growing on top of each other have regular sawtooth boundaries in some cases (Fig.6, *e*). The crystal surfaces are smooth. In one place there is a mechanical dent with a characteristic conchoidal fatigue fracture surface (Fig.6, *f*). The pits and irregularities of intergrowths on the diamond surface are sometimes covered with clay aluminosilicates and iron oxyhydroxides.

The structural belonging of a mineral grain to diamond was determined using Raman spectroscopy. The Raman spectrum of diamond obtained by excitation with a red laser (λ_{ex} = 633 nm) clearly shows an intense diagnostic peak at 1332 cm^{-1} of the main Raman active vibration, and weak peaks at 1724, 3317, and 4772 cm^{-1} are also visible (Fig.7, *a*).

The structural characteristics of the studied diamond mineral grain, obtained by X-ray photometry using the Debye – Sherrer method, demonstrate reflections of reflective planes (hkl) typical for diamond with the corresponding interplanar distances D_{hkl} (Å): 2.059 (111), 1.266 (220), 1.076 (311). The resulting debyogram shows strokes (sparse dashed lines), indicating the presence of blockiness (texturing) in the diamond. The diamond spectra obtained using a green laser (λ_{ex} = 488 nm) are a superposition of Raman and laser luminescence (LL) spectrum. The Raman spectrum includes a narrow peak at 522 nm (1322 cm^{-1}) associated with the fundamental vibration of diamond (Fig.7, *b*).

Journal of Mining Institute. 2023. Vol. 264. P. 842-855

The LL spectrum superimposed on it captures narrow resonance lines and modes of phonon repeat systems of impurity nitrogen defects in the mineral structure. The LL spectrum contains an H3 system with a weak phonon-free line at 504 nm (Fig.7, *b*). The defect responsible for the emission in this spectral region, according to modern concepts [39], consists of two nitrogen atoms that captured a vacancy and has an N_2V type structure. H3 centers are found in diamonds, which contain optically active A-defects in the crystal structure, consisting of an associated pair of nitrogen atoms located in neighboring sites of the crystal lattice. These defects are often observed in the shell parts of diamond crystals [40]. In the mineral history of the origin of natural diamond there is a stage of long stay in the mantle (mantle annealing), which results in the aggregation of impurity nitrogen, originally included inthe mineral lattice in the form of isolated single atoms – C-defects [41]. A-defects are among the simplest aggregated states of impurity nitrogen [42]. The LL spectrum of diamond also contains relatively narrow and intense lines at 527 and 541 nm, apparently also belonging to nitrogen defects.

Conclusion. In the southeastern part of the Chetlas uplift in the Middle Timan, in schlich samples taken from modern channel sediments of the river Uvyu and other nearby streams, the DSM, including chromium-bearing pyropes and chromospinelides, were found. One of the most pyrope-rich samples contained a 0.4×0.3×0.1 mm diamond grain.

The presence of pyropes and chromospinelides subjected to exogenous mechanical wear suggests that the terrigenous material in the alluvium could have come from intermediate reservoirs. Finding chromium-containing pyropes in the schlich samples, which do not have noticeable traces of mechanical wear, can be considered as signs of the close location of the primary source.

The ring structures, established within the territory under consideration are of great interest for opening the possible primary sources of diamonds. These structures are similar to those associated with tube-type geological bodies – diatremes. The main part of the identified ring structures is located in the areas of the Upper Devonian sediments, which determines the lower age boundary of formation of the objects that form them as the Late Devonian, close to the age of the kimberlites of the Arkhangelsk diamondiferous province [43-45].

The work was carried out within the framework of the state assignment of N.P.Yushkin Institute of Geology Komi SC UB RAS "*Deep structure, geodynamic evolution, geosphere interaction, magmatism, metamorphism, and isotope geochronology of the Timan-Northen Ural lithospheric segment*" *and* "*Fundamental problems of mineralogy and mineral formation, minerals as indicators of petro- and ore genesis , mineralogy of ore regions and deposits of the Timan-Northen Ural region and the Arctic territories*".

The authors are grateful to the staff of N.P.Yushkin Institute of Geology Komi SC UB RAS: *T.N.Busheneva* (*participation in field work, processing of schlich samples, isolation of heavy fraction minerals and their diagnostics*), *S.I.Isaenko* (*Raman spectroscopy, laser luminescence*), *A.S.Shuisky and E.M.Tropnikov* (*scanning electron microscopy, microprobe analysis)*, *B.A.Makeev (X-ray diffraction photometric analysis*), *V.I.Rakin* (*consultations on the crystal morphology of garnet, spinel and diamond*).

REFERENCES

1. Makeev A.B., Rybalchenko A.Ya., Dudar V.A., Shametko V.G. New perspectives of diamond-bearing Timan. Geologiya i mineralnye resursy evropeiskogo severo-vostoka Rossii. Novye rezultaty i novye perspektivy: Materialy XIII Geologicheskogo sezda Respubliki Komi. Vol. 4. Syktyvkar: Institut geologii Komi NTs UrO RAN, 1999, p. 63-66 (in Russian).

2. Malkov B.A. Geological and tectonic prerequisites for the diamond-bearing capacity of the Timan and the south-western Cis-Timan. Almazy i almazonosnost Timano-Uralskogo regiona: Materialy Vserossiiskogo soveshchaniya, 24-26 fevralya 2001, Syktyvkar, Respublika Komi, Rossiya. Syktyvkar: Institut geologii Komi NTs UrO RAN, 2001, p. 41-44 (in Russian).

3. Plyakin A.M., Shcherbakov E.S. History of studying of diamond presence of the Middle Timan. Almazy i blagorodnye metally Timano-Uralskogo regiona: Materialy Vserossiiskogo soveshchaniya, 14-17 noyabrya 2006, Syktyvkar, Respublika Komi, Rossiya. Syktyvkar: Institut geologii Komi NTs UrO RAN, 2006, p. 114-117 (in Russian).

4. State geological map of the Russian Federation of scale 1:1000000 (third generation). Mezen series. Sheet Q-39 (Naryan-Mar). Obyasnitelnaya zapiska. Gl. nauch. redaktor K.E.Yakobson. Saint Petersburg: VSEGEI, 2015, p. 517 (in Russian).

5. Makeev A.B., Lebedev V.A., Braynchaninova N.I. Magmatics of Middle Timan. Ekaterinburg: Ural Branch of RAS, 2008, p. 348 (in Russian).

6. Shumilova T.G., Filippov V.N., Kablis G.N. Graphite and its pseudomorphoses on diamond in carbonatites of the Kosyu massif (Timan). Almazy i blagorodnye metally Timano-Uralskogo regiona: Materialy Vserossiiskogo soveshchaniya 14-17 noyabrya 2006, Syktyvkar, Respublika Komi, Rossiya. Syktyvkar: Institut geologii Komi NTs UrO RAN, 2006, p. 137-138 (in Russian).

7. Shilov L.P., Plyakin A.M., Alekseev V.I. et al. Timan ridge. Monograph in 2 vol. Ukhta: Ukhtinskii gosudarstvennyi tekhnicheskii universitet, 2011. Vol. 2, p. 339 (in Russian).

8. Udoratina O.V., Andreichev V.L., Travin A.V., Savatenkov V.M. Middle Timan basalts: Rb-Sr, Sm-Nd, and Ar-Ar data. Geologiya i mineralnye resursy Evropeiskogo Severo-Vostoka Rossii: Materialy XVI Geologicheskogo sezda Respubliki Komi, 15-17 aprelya 2014, Respublika Komi, Rossiya. Syktyvkar: Institut geologii Komi NTs UrO RAN, 2014. Vol. II, p. 128-131 (in Russian).

9. Udoratina O.V., Travin A.V., Kulikova K.V., Varlamov D.A. Manifestation of Early Permian Pulse of Ultrapotassic Magmatism in Middle Timan. *Bulletin of Moscow society of naturalists. Geological series.* 2016. Vol. 91. Iss. 2-3, p. 29-35 (in Russian).

10. Golubeva I.I., Remizov D.N., Kulikova K.V. et al. Geology and composition of high-potassium trachytes of explosive subvolcanic facies of Middle Timan. *Bulletin of Moscow Society of Naturalists. Geological Series.* 2016. Vol. 91. Iss. 2-3, p. 36-46 (in Russian).

11. Udoratina O.V., Burtsev I.N., Nikulova N.Yu., Khubanov V.B. Age of Upper Precambrian metasandstones of Chetlas Group of Middle Timan on U-Pb dating of detrital zircons. *Bulletin of Moscow Society of Naturalists. Geological Series.* 2017. Vol. 92. Iss. 5, p. 15-32 (in Russian).

12. Soboleva A.A., Andreichev V.L., Burtsev I.N. et al. Detrital Zircons from Upper Precambrian Rocks of the Vym Group of Middle Timan (U-Pb Age and Provenance). *Bulletin of Moscow Society of Naturalists. Geological Series.* 2019. Vol. 94. Iss. 1, p. 3-16 (in Russian).

13. Brusnitsyna E.A., Ershova V.B., Khudoley A.K. et al. Age and Provenance of the Riphean Rocks of the Chetlas Group of the Middle Timan: U-Th-Pb (LA-ICP-MS) Dating of Detrital Zircons. *Stratigraphy and Geological Correlation.* 2021. Vol. 29. N 6, p. 607-626 (in Russian). DOI: 10.31857/S0869592X21060028

14. Makeyev A.B., Bayanova T.B., Borisovskiy S.E., Zhilicheva O.M. Composition, the U-Pb Isotope Age and Source of Zircon in the Ichetju Polymineral Occurrence (the Middle Timan). *Proceedings of the Russian Mineralogical Society*. 2015. Vol. 144. N 6, p. 9-18 (in Russian).

15. Glukhov Yu.V., Makeev B.A., Varlamov D.A. et al. Chromespinelides with zinc-bearing epigene rims from Devonian conglobreccia horizons of Ichet'yu placer-like occurrence (Middle Timan). *Lithosphere.* 2015. N 2, p. 103-120 (in Russian).

16. Isaenko S.I. Spectroscopic characteristics of diamonds from the Ichetyu placer (Middle Timan). Syktyvkar: Institut geologii Komi NTs UrO RAN, 2016, p. 102 (in Russian).

17. Makeyev A.B., Skublov S.G. Y–REE-Rich zircons of the Timan region: Geochemistry and economic significance. *Geochemistry International.* 2016. Vol. 54. N 9, p. 788-794. DOI: 10.7868/S0016752516080070

18. Makeev A.B., Krasotkina A.O., Skublov S.G. New data on U-Pb-age and geochemistry of zircon (SHRIMP-II, SIMS) from Ichetu occurrence (Middle Timan). *Vestnik of Institute of Geology of Komi Science Center of Ural Branch RAS.* 2017. N 11, p. 28-42 (in Russian). DOI: 10.19110/2221-1381-2017-11-28-42

19. Krasotkina A.O., Machevariani M.M., Korolev N.M. et al. Typomorphic Features of Niobium Rutile from the Polymineral Occurrence Ichetju (The Middle Timan). *Proceedings of the Russian Mineralogical Society.* 2017. Vol. 146. N 2, p. 88-100 (in Russian).

20. Grakova O.V. Diamond occurrences of the Middte and South Timan. Syktyvkar: Institut geologii Komi NTs UrO RAN, 2021, p. 144 (in Russian). DOI: 10.19110/89606-021

21. Bogatikov O.A., Garanin V.K., Kononova V.A. et al. Arkhangelsk diamondiferous province. Moscow: Moskovskiy gosudarstvennyy universitet, 1999, p. 524 (in Russian).

22. Savko A.D., Shevyrev L.T., Ilyash V.V., Chashka A.I. New Occurences of the High-pressure Minerals of the Voronezh Anteclise Sedimentary Mantle – Implication for the Diamond Host Sources Discovery. *Proceedings of Voronezh State University. Series: Geology.* 2007. N 1, p. 43-74 (in Russian).

23. Shchukina E.V., Agashev A.M., Pokhilenko N.P. Metasomatic origin of garnet xenocrysts from the V. Grib kimberlite pipe, Arkhangelsk region, NW Russia. *Geoscience Frontiers*. 2017. Vol. 8. Iss. 4, p. 641-651. DOI: 10.1016/j.gsf.2016.08.005

24. Sobolev N.V., Logvinova A.M., Tomilenko A.A. et al. Mineral and fluid inclusions in diamonds from the Urals placers, Russia: Evidence for solid molecular N_2 and hydrocarbons in fluid inclusions. *Geochimica et Cosmochimica Acta*. 2019. Vol. 266, p. 197-219. DOI: 10.1016/j.gca.2019.08.028

25. Proskurnin V.F., Grakhanov S.A., Petrov O.V. et al. Forecast of the diamond potential of Taimyr. *Doklady RAN. Nauki o Zemle.* 2021. Vol. 499. N 2, p. 97-102 (in Russian). DOI: 10.31857/S2686739721080107

26. Ustinov V.N., Mikoev I.I., Piven G.F. Prospecting models of primary diamond deposits of the north of the East European Platform. *Journal of Mining Institute.* 2022. Vol. 255, p. 299-318. DOI: 10.31897/PMI.2022.49

27. Simakov S.K., Stegnitskiy Y.B. On the presence of the postmagmatic stage of diamond formation in kimberlites. *Journal of Mining Institute.* 2022. Vol. 255, p. 319-326. DOI: 10.31897/PMI.2022.22

28. Bushenev A.A., Pystin A.M. On the perspective of identifying the bed-rocks sources of diamonds in the Chetlas-Obdyrsk uplift (Middle Timan). *Geodinamika, veshchestvo, rudogenez Vostochno-Evropeiskoi platformy i ee skladchatogo obramleniya.* Syktyvkar: Institut geologii Komi NTs UrO RAN, 2017, p. 36-37 (in Russian).

29. Antonova I.B. Method of searching for explosion tubes in the conditions of the developed sedimentary cover of the North-West of the USSR on the materials of remote surveys. *Printsipy i metodika distantsionnykh issledovanii pri prognozirovanii tverdykh poleznykh iskopaemykh*. Saint Petersburg: VSEGEI, 1992, p. 144 (in Russian).

30. Pystin A.M., Glukhov Y.V., Bushenev A.A. New Findings of Diamonds and Diamond Indicator Minerals in the Middle Timan and Prospects of the Search for Their Original Sources. *Doklady Earth Sciences*. 2021. Vol. 497. N 1, p. 232-236 (in Russian). DOI: 10.31857/S2686739721010187

31. Afanasev V.P., Zinchuk N.N., Pokhilenko N.P. Morphology and morphogenesis of kimberlite indicator minerals. Novosibirsk: Filial "Geo" Izdatelstva SO RAN, Izdatelskii dom "Manuskript", 2001, p. 276 (in Russian).

32. Agashev A.M., Ionov D.A., Pokhilenko N.P. et al. Metasomatism in lithospheric mantle root: Constraints from whole-rock and mineral chemical composition of deformed peridotite xenoliths from kimberlite pipe Udachnaya. *Lithos*. 2013. Vol. 160-161, p. 201-215. DOI: 10.1016/j.lithos.2012.11.014

33. Howarth G.H., Barry P.H., Pernet-Fisher J.F. et al. Superplume metasomatism: Evidence from Siberian mantle xenoliths. *Lithos*. 2014. Vol. 184-187, p. 209-224. DOI: 10.1016/j.lithos.2013.09.006

34. Pokhilenko N.P., Agashev A.M., Litasov K.D., Pokhilenko L.N. Carbonatite Metasomatism of Peridotite Lithospheric Mantle: Implications for Diamond Formation and Carbonatite-Kimberlite Magmatism. *Russian Geology and Geophysics*. 2015. Vol. 56. N 1-2, p. 280-295.

35. Sobolev N.V. The Deep Seated Inclusions in Kimberlites and the Problem of the Upper Mantle Composition. Novosibirsk: Nauka, 1974. 264 p (in Russian).

36. Pavlov N.V. Chemical composition of chrome spinels in connection with the petrographic composition of rocks of ultrabasic intrusives. *Trudy instituta geologicheskikh nauk AN SSSR. Seriya rudnykh mestorozhdenii*. 1949. Iss. 103. N 13, p. 3-88 (in Russian).

37. Barnes S.J., Roeder P.L. The Range of Spinel Compositions in Terrestrial Mafic and Ultramafic Rocks. *Journal of Petrology*. 2001. Vol. 42. Iss. 12, p. 2279-2302. DOI: 10.1093/petrology/42.12.2279

38. Roeder P.L., Schulze D.J. Crystallization of Groundmass Spinel in Kimberlite. *Journal of Petrology*. 2008. Vol. 49. Iss. 8, p. 1473-1495. DOI: 10.1093/petrology/egn034

39. Vins V.G. Changing the color of brown natural diamonds under the influence of high pressures and temperatures. *Zapiski Vserossiiskogo mineralogicheskogo obshchestva*. 2002. Vol. 131. N 4, p. 111-121 (in Russian).

40. Vasilev E.A. Defects of diamond crystal structure as an indicator of crystallogenesis. *Journal of Mining Institute.* 2021. Vol. 250, p. 481-491. DOI: 10.31897/PMI.2021.4.1

41. Evans T. Aggregation of Nitrogen in Diamond. The Properties of Natural and Synthetic Diamond. London: Academic Press, 1992, p. 259-290.

42. Stepanov A.S., Shatsky V.S., Zedgenizov D.A., Sobolev N.V. Causes of Variations in Morphology and Impurities of Diamonds from the Udachnaya Pipe Eclogite. *Russian Geology and Geophysics.* 2007. Vol. 48. N 9, p. 758-769.

43. Mahotkin I.L., Gibson S.A., Thompson R.N. et al. Late Devonian Diamindiferous Kimberlite and Alkaline Picrate (Protokimberlite?) Magmatism in the Archangelsk Region, NW Russia. *Journal of Petrology*. 2000. Vol. 41. Iss. 2, p. 201-227. DOI: 10.1093/petrology/41.2.201

44. Pervov V.A., Bogomolov E.S., Levskii L.K. et al. Rb-Sr Age of Kimberlites of the Pionerskaya Pipe, Arkhangelsk Diamondiferous Province. *Doklady Earth Sciences*. 2005. Vol. 400. N 1, p. 67-71.

45. Larionova Y.O., Sazonova L.V., Lebedeva N.M. et al. Kimberlite Age in the Arkhangelsk Province, Russia: Isotopic Geochronologic Rb-Sr And $^{40}Ar/^{39}Ar$ and Mineralogical Data on Phlogopite. *Petrology.* 2016. Vol. 26. N 6, p. 607-639. DOI: 10.7868/S0869590316040026

***Authors*: Aleksandr M. Pystin,** *Doctor of Geological and Mineralogical Sciences*, *Head of Laboratory*, *pystin@geo.komisc.ru*, *https://orcid.org/0000-0002-5875-4353* (*N.P.Yushkin Institute of Geology Komi SC UB RAS*, *Syktyvkar*, *Russia)*, **Yurii V. Glukhov,** *Candidate of Geological and Mineralogical Sciences*, *Senior Researcher*, *https://orcid.org/0000-0002-2633-0636* (*N.P.Yushkin Institute of Geology Komi SC UB RAS*, *Syktyvkar*, *Russia*), **Aleksandr A. Bushenev,** *Head of Department*, *https://orcid.org/0009-0007-1708-5732* (*Republican Center for the Functioning of Specially Protected Natural Areas and Nature Management*, *Syktyvkar*, *Russia*).

The authors declare no conflict of interests.